Monte Carlo study of thermodynamic properties and clustering in the bcc Fe-Cr system

M. Yu. Lavrentiev,[1,*] R. Drautz,[2] D. Nguyen-Manh,[1] T. P. C. Klaver,[3] and S. L. Dudarev[1,4]
[1]*EURATOM/UKAEA Fusion Association, Culham Science Centre, Oxfordshire OX14 3DB, United Kingdom*
[2]*Department of Materials, University of Oxford, Parks Road, Oxford OX1 3PH, United Kingdom*
[3]*School of Mathematics and Physics, Queen's University Belfast, Belfast BT7 1NN, Northern Ireland, United Kingdom*
[4]*Department of Physics, Imperial College, Exhibition Road, London SW7 2AZ, United Kingdom*
(Received 28 July 2006; revised manuscript received 21 November 2006; published 17 January 2007)

Iron-chromium alloys are characterized by a complex phase diagram, by the small negative enthalpy of mixing at low Cr concentrations in the bcc α-phase of Fe, and by the inversion of the short-range order parameter. We present Monte Carlo simulations of the binary Fe-Cr alloy based on the cluster expansion approximation for the enthalpy of the system. The set of cluster expansion coefficients is validated against density functional calculations of energies of small clusters of chromium in bcc structure. We show that in the limit of small Cr concentration the enthalpy of mixing remains negative up to fairly high temperatures, and individual Cr atoms remain well separated from each other. Clustering of Cr atoms begins at concentrations exceeding approximately 10% at 800 K and 20% at 1400 K, with Cr-Fe interfaces being parallel to the [110] planes. Calculations show that the first and the second short-range order parameters change sign at approximately 10.5% Cr, in agreement with experimental observations. Semi-grand-canonical ensemble simulations used together with experimental data on vibrational entropy of mixing give an estimate for the temperature of the top of the α-α' miscibility gap. We find that the complex ordering reactions occurring in Fe-Cr, as well as the thermodynamic properties of the alloy, can be reasonably well described using a few concentration-independent cluster expansion coefficients.

DOI: 10.1103/PhysRevB.75.014208 PACS number(s): 64.75.+g, 61.46.Bc, 61.43.−j, 82.60.Lf

I. INTRODUCTION

Fundamental materials research involving both experiments and theoretical simulations and aimed at the development of advanced materials is widely recognized as one of the key elements of design of new energy generation facilities.[1–5] A serious challenge in the field of materials for fusion and generation IV fission reactors is the development of alloys capable of performing reliably for a long time under extreme conditions, including high irradiation levels (total dose of 50–200 dpa) and high temperature (up to 1000 °C). The first wall materials for fusion power plants must also have adequate mechanical strength, ductility, toughness, and resistance to corrosion. The two alloy systems currently under investigation are the low-activation ferritic/martensitic steels typically containing 8–9% Cr, and the nanocomposite ferritic alloys containing 13±2% Cr.[6–9] Hence a full understanding of thermodynamic and mechanical properties of iron-chromium alloys in the limit of relatively low (up to 16–20%) Cr content is of particular significance for applications.

The phase diagram of the Fe-Cr binary system is fairly complex. It includes the fcc γ-phase (γ-loop) forming at temperatures above 830 °C for Cr concentration below 12%, and the fairly complex (containing 30 atoms in a unit cell) σ-phase occurring at temperatures between 500 °C and 820 °C for Cr concentrations around 50%.[10–13] The range of operational temperatures of a prospective fusion power plant corresponds to the low-temperature part of the phase diagram, where the ferromagnetic bcc α-phase remains stable. This important region, which includes a large miscibility gap separating the Fe-rich α-phase and the Cr-rich α'-phase, is the subject of this paper. Experimentally it is more difficult to access this part of the phase diagram than the high-temperature region, since lowering the temperature results in a much longer time required to reach equilibrium. In many cases this period of time exceeds the time available to experimental observations, and this makes comparison with modeling studies particularly significant. Our paper describes a Monte Carlo investigation of thermodynamic properties of the bcc phase of the FeCr system based on a density functional theory (DFT)-derived cluster expansion (CE) Hamiltonian. We consider this work as the first step toward calculating the low-temperature phase diagram of the Fe-Cr binary system.

Recent advances in density functional theory have made it possible to perform calculations of the energy of clusters containing several hundreds of atoms, enabling the accurate comparison of enthalpies of formation of disordered atomic configurations. On the basis of these calculations the cluster expansion formalism introduced and developed some time ago[14,15] has been extended to surfaces[16] and magnetic systems[17] and applied to the evaluation of the thermodynamics properties of a variety of systems, including magnetic alloys.[18,19] In this paper, we use DFT calculations to define a set of coefficients for a CE Hamiltonian describing interactions between iron and chromium atoms in a defect-free binary alloy.

Monte Carlo (MC) simulations are widely used for calculating statistical properties of liquids and elemental solids. In recent years, the development of new computational methods accompanied by continuing growth in computer power has led to a rapidly increasing contribution of computer simulation to modeling solid solutions. Until recently, the main difficulty was associated with the extremely long computation time (associated with the high potential energy barrier separating configurations) needed to transform one configuration

into another. This problem was finally overcome several years ago with the development of the Monte Carlo Exchange (MCX) algorithm[20,21] that, in addition to the usual MC steps involving random displacements of atoms or a random change in size of the simulation box, also includes random exchanges of atoms of two different types. Just as in a conventional MC algorithm, the Metropolis algorithm[22] is applied to determine whether an attempt is accepted or rejected. The method allows fast sampling of configurations for systems where atoms of different types are similar in size and in terms of the character of interatomic interactions. Recently the method has been extended to the case where the atoms in a solution have strongly different properties.[23] The MCX algorithm was successfully applied, among other problems, to studying ceramics,[21,23] spinels,[24] garnets,[25] metal alloys,[26,27] and surface segregation.[28] In this study, we apply the MCX method to investigate thermodynamic properties of the Fe-Cr binary alloy in the cluster expansion approximation.

By combining *ab initio* calculations with the cluster expansion and MC simulations, we first use the results of CE-based Monte Carlo simulations to validate and verify the cluster expansion coefficients derived initially from the *ab initio* density functional data. The validated set of the CE coefficients is then used to perform MC simulations for a large supercell and to study the relative energies of configurations and the effects of ordering and clustering occurring in the binary Fe-Cr alloy at different concentrations and temperatures. We investigate the enthalpy of mixing, the short-range order parameters, and the size and the shape of Cr clusters in iron. The paper is organized as follows: in Sec. II we discuss methods of calculation and details of the computational approach. Results are described in Sec. III of the paper and are summarized in Sec. IV.

II. METHODOLOGY

A. The cluster expansion method

The cluster expansion (CE) method is a way of representing the energy (or the enthalphy provided that the external pressure is zero) of configurations of atoms on a lattice.[14] It is a convenient and efficient tool for studying properties of solid solutions over a wide range of concentrations and temperatures. For binary systems, we introduce the so-called occupation variable $\sigma=+1(-1)$ that indicates whether a lattice site is occupied by an atom of type A or B, respectively (in this study we choose +1 for Fe and −1 for Cr). A configuration i defined on a lattice with N sites is characterized by a vector of occupation variables $\vec{\sigma}_i=\{\sigma_1,\sigma_2,\ldots,\sigma_N\}$. The CE method postulates that the enthalpy of the crystal can be represented in the form

$$E(\sigma_i)=J_0+\sum_\alpha D_\alpha J_\alpha \Phi_\alpha(\sigma_i), \tag{1}$$

where the cluster functions $\Phi_\alpha(\sigma_i)$ are expressed as products of occupation variables associated with a given cluster α in a configuration i, J_α are the cluster expansion coefficients (ECIs), and the degeneracy factors D_α give the number of clusters that are equivalent in terms of their symmetry. In a real alloy the small difference between atomic radii of different atoms gives rise to local distortions of the lattice. However, this does not change the topology of the bcc structure and hence, the cluster coefficients effectively map the actual relaxed atomic lattice configurations onto a perfect crystal lattice. In this way small elastic distortions are included in the cluster expansion coefficients. In the case considered in the paper this is justified by the very small difference between the sizes of an iron and a chromium atom. In principle, the CE method can take into account the elastic interactions explicitly (see, e.g., Ref. 15).

The ECIs may be obtained from a database of *ab initio* DFT total energy calculations for describing various occupation configurations by means of the numerical inversion of Eq. (1). In this paper we employ the variational CE,[29] which was shown to provide stable and robust numerical values for the ECIs.[29–31] We imposed conditions $J_0=0$, $J_1=0$ on the cluster expansion coefficients used in this work.[16] The first condition is consistent with the assumption that the enthalpy of mixing of pure elements on both ends of the phase diagram is zero, and the second represents a measure of the difference between Fe and Cr. However, the choice $J_1=0$ is immaterial for the results obtained in this paper, since the numbers of atoms of both types remain constant in a simulation. There are methods, such as transmutational ensemble Monte Carlo, where the numbers of Fe and Cr atoms vary during the simulation. In this case, the choice of value for J_1 does influence the results of simulations.

To find the cluster expansion coefficients for the Fe-Cr alloy we used a database of 74 input structures.[32] This database focused mostly on the Fe-rich range of configurations but also included some structures with higher Cr content to make sure that the CE coefficients contain information about the entire range of Cr concentrations. In Ref. 32 it was shown that in order to describe energies of the Fe-Cr system at the meV level of accuracy, large many-body clusters had to be included in the cluster expansion. Our initial choice of cluster expansion set of 24 compact clusters on the bcc lattice resulted in predictive error of ~4 meV/atom. However, several trial structures not included in the initial database and discovered in trial MC simulations were found to have energies outside this interval of uncertainty. We therefore decided to adopt a balanced approach where, at the expense of somewhat larger predictive error, we retained higher confidence in the predictive capability of the method. Since it is not the aim of this paper to reproduce the energy landscape of Fe-Cr with meV accuracy but rather to show how the ordering in Fe-Cr may be described with a few concentration-independent expansion coefficients, we reduced the initial set of cluster expansion coefficients[29] to only 12 clusters. The accuracy of this set of CE coefficients is limited by a conservative predictive error of ~7 meV/atom, which is comparable with the lowest (negative) enthalpy of mixing found in the *ab initio* calculations of Fe-Cr. We are continuing to extend the DFT database of the Fe-Cr bcc system.[33,34] By using this extended database, we should be able to modify and improve the numerical values of the CE coefficients and reduce the predictive error for the entire range of concentrations.

B. Monte Carlo simulations

Monte Carlo simulations, together with the cluster variation method (CVM), are the two commonly used methods for studying thermodynamics of systems with configurational disorder (examples of the application of the CVM technique in the CE approximation are given in Refs. 35 and 36). CE-based CVM has the advantage of giving an explicit analytical expression for the configurational entropy. In the CE-based MC, calculating the entropy and the free energy is less straightforward. On the other hand, in the limit of a large size of clusters the CE-based analytical expressions become more cumbersome. Also, MC is better suited for studying microscopic properties, such as clustering and formation of precipitates. On balance, in this study we decided to choose CE-based Monte Carlo as a method of simulation of the FeCr system.

In simulations of nonstoichiometric solid solutions based on conventional MC, kinetic barriers do not allow sampling of the entire space of configurations since the algorithm leads to confinement in the vicinity of the initial configuration. The first attempt to overcome this difficulty was made by Kawasaki,[37,38] who introduced the nearest-neighbor spin exchange. Since then, Monte Carlo exchange simulations (see, e.g., Refs. 20 and 21) became the method of choice for simulating systems with configurational disorder. In MCX, explicit changes of atomic configurations are allowed. In an event, a random choice is made regarding whether to attempt a random exchange between a pair of (different) atoms, or a random displacement of an atom, or a random change in the volume of the simulation box. The decision whether to accept or to reject the move is made according to the standard Metropolis scheme,[22] namely, if the energy change $\Delta U = U_{final} - U_{initial}$ is negative, the move is accepted, and if ΔU is positive, the move is accepted with the probability

$$p = \exp\{-\beta \Delta U\}, \quad \beta = \frac{1}{kT}, \tag{2}$$

where k is the Boltzmann constant and T is the absolute temperature. This approach makes an atomic configuration evolve during a simulation. In the current version of the cluster expansion approximation, MCX is the only Monte Carlo method suitable for carrying out the simulation, since atoms move on a fixed lattice, making an application of conventional MC involving movements of atoms and changes in the volume of simulation box impossible (note that in other versions of the CE approach that include the constituent strain energy, additional types of Monte Carlo moves can be introduced). MCX makes it possible to calculate the enthalpy of mixing, the short-range order parameters, and the shape and the size of precipitates of one phase in another (e.g., the shape of Cr clusters forming in the α-phase).

Calculating the free energy of the system and, consequently, the phase diagram in the Monte Carlo scheme is less straightforward. Absolute values of the free energy cannot be determined from Monte Carlo calculations. However, the recently developed methods allow calculation of the *variation* of the free energy as a function of concentration that can be used to make estimates related to the general properties of the phase diagram. In this paper we describe an application of one of such methods, namely, the semi-grand-canonical ensemble simulations of the Fe-Cr system. In this method[21,39,40] we evaluate the derivative of the Gibbs free energy G with respect to concentration, related to the difference in the chemical potentials between the species,

$$\left(\frac{\partial G(x_{\mathrm{Cr}})}{\partial x_{\mathrm{Cr}}}\right) = \mu_{\mathrm{Cr}} - \mu_{\mathrm{Fe}}. \tag{3}$$

To achieve this, we first evaluate the change in the potential energy $\Delta U_{\mathrm{Cr/Fe}}$ associated with the conversion of one of the species, for example, Cr, into another, in this case Fe. This change in the energy of the system is related to the difference between chemical potentials $\Delta\mu = \mu_{\mathrm{Cr}} - \mu_{\mathrm{Fe}}$ via

$$\Delta\mu = -kT\left\langle \frac{N_{\mathrm{Cr}}}{N_{\mathrm{Fe}}+1} \exp(-\Delta U_{\mathrm{Cr/Fe}}/kT) \right\rangle \tag{4}$$

[for a derivation of (4) see Ref. 40 and references therein]. In this way we evaluate the energy associated with the conversion of a randomly chosen Cr atom into a Fe atom in a simulation. Note that this change is only hypothesized but not actually performed—the configuration remains unchanged after evaluating $\Delta U_{\mathrm{Cr/Fe}}$, and the simulation continues as before.

Most of the Monte Carlo simulations reported in this paper were performed on a simulation box consisting of $40 \times 40 \times 40$ bcc unit cells (128 000 atoms) using periodic boundary conditions, with convergence checks performed using larger supercells containing $60 \times 60 \times 60$ or $80 \times 80 \times 80$ unit cells (432 000 or 102 4000 atoms, respectively). Monte Carlo runs consisted of 10^8 exchange attempts in both the equilibration and accumulation stages (3125 exchange attempts per atom). The simulations with decreasing temperature described in Sec. III A were performed on a small $4 \times 4 \times 4$ supercell to cross-check (in the CE approximation) the results of DFT calculations performed using small supercells.

III. RESULTS

A. Validation of cluster expansion coefficients

As a first step, we checked and validated the set of CE coefficients by calculating the enthalpy of mixing of the FeCr system for a number of concentrations in a $4 \times 4 \times 4$ supercell. The low-energy configurations were found by cooling down, from 2000 K to 0 K, an initially random binary alloy configuration. We then compared our results, representing the mixing enthalpy as a function of Cr concentration, with our own DFT data[32–34] and with the data given by Olsson *et al.*[41,42] DFT calculations consistently predict negative values for the enthalpy of mixing for the range of low Cr concentrations. The mixing enthalpy changes sign as the Cr concentration increases and is positive everywhere above ~10–12% Cr. Despite including only a small set of 12 clusters, the cluster expansion shows good agreement with DFT, exhibiting negative enthalpy of mixing only in the limit of low Cr concentrations <12%. All the Monte Carlo simulations described in this paper were performed using this 12-

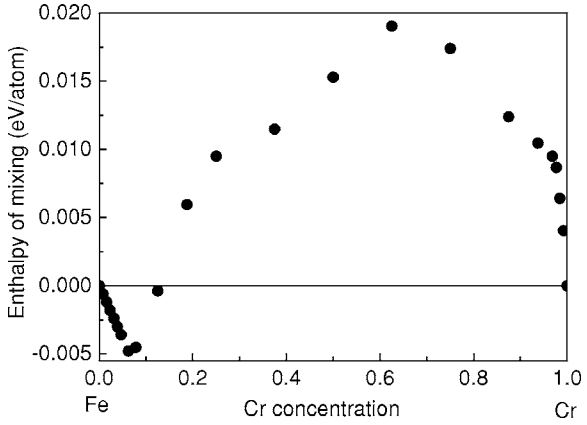

FIG. 1. Lowest enthalpies of mixing (eV/atom) of the FeCr system found by simulated annealing of $4\times4\times4$ supercells in the CE approximation vs Cr concentration.

cluster set. Figure 1 shows the lowest mixing enthalpies obtained by simulated annealing of $4\times4\times4$ supercells as a function of Cr concentration. The 12 clusters of the set are shown in Fig. 2(a) and the values of CE coefficients are summarized in Table I. Also, the values of CE coefficients for the first ten clusters are given Fig. 2(b) (note that only three two-body coefficients are shown in Fig. 2(b), given that second- and third-nearest neighbor two-body coefficients are negligibly small, see Table I). We would like to emphasize the contribution of different CE coefficients to the shape of the enthalpy of mixing curve (Fig. 1). The change in the sign of all the occupation variables σ_i in the system does not change the form of cluster functions $\Phi_\alpha(\sigma_i)$ for clusters that include an even number of atoms (two- and four-atom clusters, in the current CE set). As a result, the even-sized clusters can only lead to a symmetric enthalpy of mixing curve. The three- and five-atom clusters are responsible for the asymmetrical shape of the curve. In particular, the presence of a range of concentrations with negative enthalpy of mixing at low Cr concentrations and the positive enthalpy of mixing in the limit of high Cr concentration can only be achieved via clusters with an odd number of atoms. However, we found that a large negative coefficient of −46.18 meV, corresponding to the nearest-neighbor two-atom cluster (cluster 1, see Table I) in the absence of longer-ranged two-atom CE coefficients, results in a large and positive contribution to the enthalpy of mixing throughout the entire concentration range (up to ~90 meV/atom), so that longer-range two-atom clusters are required in order to decrease the enthalpy of mixing and to change the sign of the enthalpy of mixing for low chromium concentrations.

B. The enthalpy of mixing

It was shown in Ref. 32 that the negative enthalpy of mixing corresponding to the range of low Cr concentrations results from the negative heat of solution of single Cr atoms. At short distances Cr atoms in iron repel each other. The strong nearest-neighbor repulsion between Cr atoms is probably related to magnetic frustration. It is magnetism that inhibits the formation of Cr-rich phases at concentrations up to

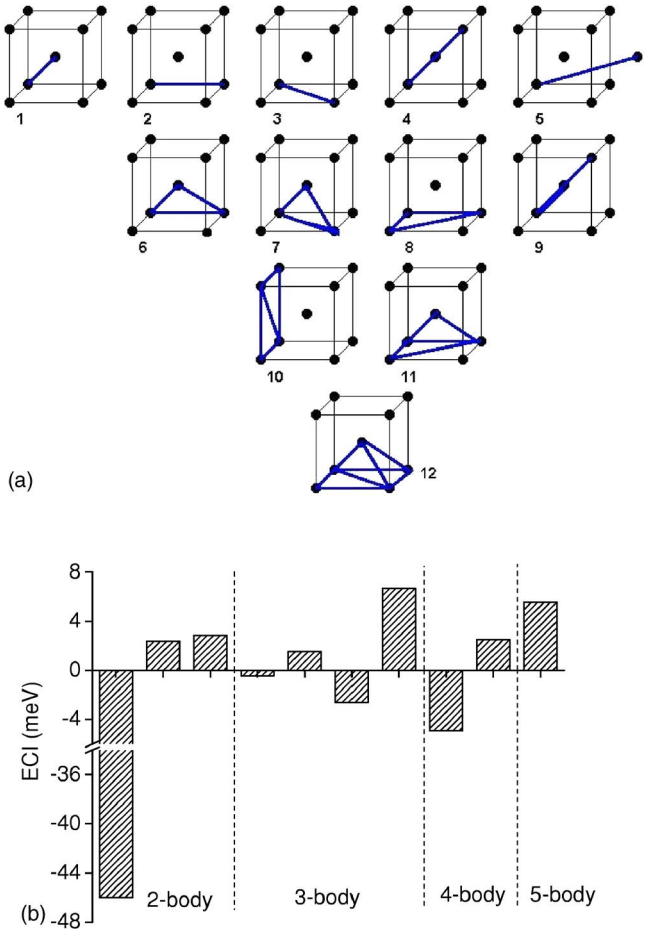

FIG. 2. (Color online) Schematic view of the clusters included in the CE used in this paper (a) and the values of the CE coefficients (b). Only three two-body coefficients are shown in Fig. 2(b). The second- and the third-nearest-neighbor two-body coefficients are negligibly small in comparison (see Table I).

10–12% Cr, and the lowest energy configurations in that range of concentration correspond to Cr atoms being surrounded by iron atoms, with Cr-Cr distances being as large as possible. These findings are confirmed by the investigation of the magnetic properties of the Fe-Cr system.[34] In particular, antiferromagnetic interactions between an isolated Cr atom and the host iron matrix, and the formation of a short-range ordered FeCr configuration (see below) both contribute to the negative enthalpy of mixing. The cluster expansion reproduces these features of Cr-Cr and Cr-Fe interactions, even if it does not explicitly include magnetic interactions. In our $4\times4\times4$ supercell (128 atoms) calculations, the lowest energy structures for systems containing up to 8 Cr atoms (6.25% Cr) were such that Cr atoms were not closer than the 6th nearest neighbor to each other (i.e., the Cr-Cr distance was greater than or equal to $2a$, where a is the bcc lattice constant). The structure of the 6.25% Cr ordered configuration found in the current MC simulations [Fig. 3(a)] is identical to one of the structures predicted earlier by DFT calculations within the Fe-Cr bcc database.[33,34] The enthalpy of mixing predicted for this structure by DFT is also negative and equals −6.5 meV/atom, with Cr atoms aligned antiferro-

TABLE I. The set of CE coefficients used in the paper (in eV). NN=nearest neighbor. Number of the coefficient corresponds to the number of the cluster in Fig. 2(a).

Number of atoms in cluster	CE coefficients (meV)
2	(1) −46.18 (NN)
	(2) 0.00039 (NNN)
	(3) 0.001 (3rd NN)
	(4) 2.35 (4th NN)
	(5) 2.85 (5th NN)
3	(6) −0.46
	(7) 1.52
	(8) −2.62
	(9) 6.66
4	(10) −4.95
	(11) 2.49
5	(12) 5.53

magnetically to the Fe atoms in the cell. For concentrations below 6.25% Cr (i.e., for supercells containing less than 8 Cr per a 128-atom supercell) the enthalpy of mixing found in our MC simulations decreases linearly as a function of Cr concentration. This is because in this case it is possible for Cr atoms to disperse in the Fe matrix, keeping no closer than 6th nearest neighbor distance apart from each other. At 6.25% Cr concentration the enthalpy of mixing found in MC simulations reaches the minimum value of −4.8 meV/atom.

We note that this lowest energy Fe-6.25%Cr configuration found using the CE-based analysis in not the lowest energy configuration present in the DFT database.[32] The structure corresponding to the lowest enthalpy of mixing found so far by DFT calculations[32] is shown in Fig. 3(b). The enthalpy of mixing for this configuration is −8.4 meV/atom. This structure corresponds to a Cr concentration of 7.41%, with the nearest Cr-Cr distances at the third nearest neighbor. The current set of cluster expansion coefficients predicts the enthalpy of mixing for the structure shown in Fig. 3(b) as

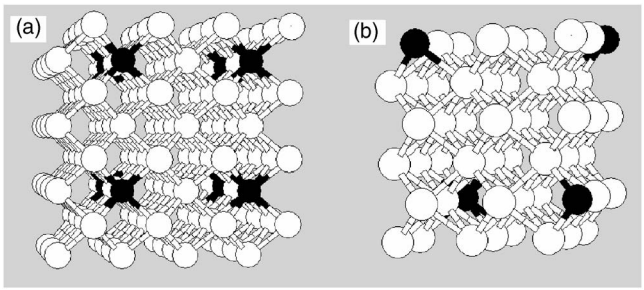

FIG. 3. The lowest enthalpy of mixing structure found in the current CE-based MC simulations for a $4\times4\times4$ supercell (a) and the lowest enthalpy of mixing structure found in DFT simulations for a $3\times3\times3$ supercell (b). Black circles denote Cr atoms, white circles Fe atoms. (a) A set of eight unit cells of the structure and (b) a single unit cell. Note that in the two structures, the first and the second nearest neighbors of a Cr atom are atoms of Fe only, and the environment of a Cr atom in the two structures differs only in the third coordination shell.

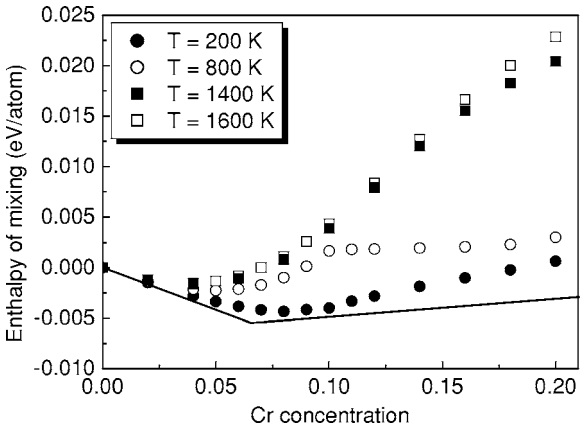

FIG. 4. The enthalpy of mixing (in eV/atom units) of the FeCr solid solution vs Cr concentration at low Cr concentrations. The straight line shows the limiting behavior of the enthalpy of mixing at $T=0$ and in the limit of an infinitely large simulation cell.

−3.0 meV/atom. The difference between the enthalpies of mixing found for this structure using DFT and CE is within the conservative predictive error of the method discussed above. Hence, while in the current set of simulations we predict the Fe-6.25%Cr structure as the lowest energy configuration, we can probably identify the finite extent of the DFT database as a possible source of error for the method.

As the Cr concentration increases from 6 to 7%, the enthalpy of mixing begins to increase. We interpret this as being due to the fact that Cr atoms no longer can be kept sufficiently far apart from each other. The enthalpy of mixing changes its sign at the point where there are 16 atoms of Cr in the supercell (12.5%) and remains positive for all the concentrations exceeding 12.5% Cr.

The validated set of CE coefficients makes it possible to perform calculations for fairly large systems and a relatively broad range of temperatures. If the enthalpy of mixing were positive everywhere, one would expect to find complete phase separation at low temperatures and the formation of a solid solution for all concentrations above a certain critical temperature. The minimum of the enthalpy of mixing gives rise to the formation of a solid solution of Cr in Fe (α-phase) for small Cr concentrations for all the temperatures, including the lowest, investigated in our simulations. At a constant temperature, as the Cr concentration increases the system undergoes a phase separation. Clusters of pure Cr (α'-phase) begin to form (see below, Sec. III D) in coexistence with the α-phase. This transition from pure α-phase to phase separation is also reflected in the change of behavior of the enthalpy of mixing treated as a function of Cr content. In Fig. 4, where the enthalpy of mixing is shown for several values of absolute temperature and Cr concentrations up to 20%, this change of behavior is seen at about 10% Cr for $T=800$ K. At even lower temperature $T=200$ K, the enthalpy of mixing remains negative for almost the entire range of concentrations shown in Fig. 4 (until 18% Cr). This is because above 6–7% Cr the alloy becomes a mixture of pure Cr, which has zero enthalpy of mixing, and the α-phase (which has a negative enthalpy of mixing). In the limit $T=0$ and an infinitely large simulation cell, the behavior of the

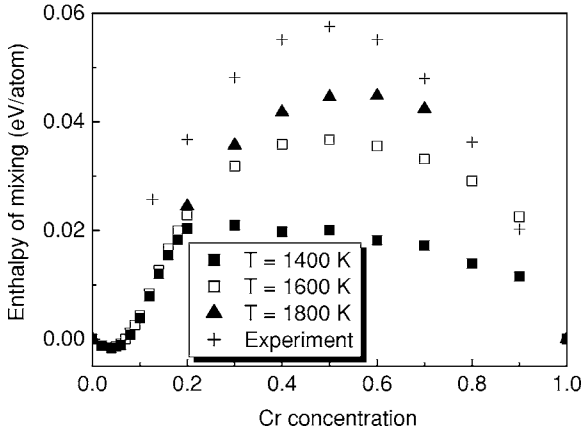

FIG. 5. The enthalpy of mixing (in eV/atom units) of the FeCr solid solution vs Cr concentration at high temperatures in the whole region of Cr concentrations, together with experimental data.[13]

enthalpy of mixing shown in Fig. 4 is given by two straight lines: one corresponding to the solid solution of Cr in the Fe matrix for concentrations lower than 6.25% Cr, and the second corresponding to the coexistence of the Fe-6.25%Cr ordered configuration described above, and pure Cr. We note that for concentrations lower than 6.25% Cr the average distance between Cr atoms exceeds the range of CE coefficients and hence, the method adopted here cannot distinguish between a solid solution phase and the possible ordered configurations of the alloy.

At high temperatures, the Boltzmann weight of high-energy configurations increases, increasing the enthalpy of mixing. In Fig. 5 we show the behavior of the enthalpy of mixing in the whole range of concentrations for high temperatures, together with experimental data corresponding to $T=1400$ K.[13] The main features of the $T=0$ K enthalpy of mixing plot (Fig. 1) remain unchanged at higher temperatures, e.g., even at $T=1600$ K the enthalpy of mixing remains negative in the limit of small Cr concentrations. However, the region of concentrations where the enthalpy of mixing is negative becomes smaller and extends at $T=1600$ K only up to 7% Cr, compared to 12% Cr for the region of negative enthalpy of mixing at $T=0$ K. Note that at $T=1600$ K and $T=1800$ K we do not see any change of behavior corresponding to the transition from a solid solution to the phase separation seen at about 20% Cr at $T=1400$ K. This suggests that the transition to complete miscibility occurs between 1400 K and 1600 K in the CE approximation adopted in this study. As expected, the enthalpy of mixing increases with temperature, improving agreement with experiment, but even at $T=1800$ K the MC results are lower than the experimental data at 1400 K. In our opinion, among the reasons for the remaining discrepancy might be the following: (i) the set of the CE coefficients was optimized mainly using the DFT data for low Cr concentrations and hence, its validity is limited when extended to the range of medium and high Cr concentrations; (ii) the effect of magnetic excitations (magnons) at elevated temperatures was not taken into account.

C. The short-range order

The short-range order (SRO) in a solid solution $Fe_{1-x}Cr_x$ can be described via the Warren-Cowley parameters $\alpha_n(x)$ (Ref. 43)

$$\alpha_n(x) = 1 - \frac{P_n^{\text{Cr-Fe}}}{1-x}, \tag{5}$$

where n is the number of a coordination sphere, and $P_n^{\text{Cr-Fe}}$ is the conditional probability of finding a Fe atom in the nth coordination sphere of Cr. The SRO parameter equals 0 if the probability $P_n^{\text{Cr-Fe}}=1-x$, i.e., if the probability coincides with the Fe content and there is no preference for the Cr atom to be surrounded by Fe or Cr (an ideal solid solution). Clustering of Cr atoms gives rise to positive values of $\alpha_n(x)$ (repulsive short-range order), while negative values of $\alpha_n(x)$ suggest a tendency toward forming an ordered structure, or attractive SRO. If at low x each Cr atom is surrounded by Fe atoms only ($P_1^{\text{Cr-Fe}}=1$), the SRO parameter α_1 takes its lowest possible value $\alpha_1^{\min}=-(x/1-x)$.

The first prediction of negative SRO parameters in Fe-Cr at small Cr concentration, resulting in the inversion of the sign at the first nearest neighbor position to positive at about 25% Cr, was made by Hennion in 1983.[44] One year later this effect was confirmed experimentally.[45] The actual concentration at which the inversion takes place is approximately 10% Cr. Recently, this anomaly was discussed by Caro *et al.*[46] They performed MC simulations of Fe-Cr with a classical many-body potential based on DFT calculations of the heat of solution in the coherent potential approximation (CPA) performed by Olsson *et al.*[47] The authors of Ref. 46 found that at $T=500$ K the inversion of SRO takes place at approximately 5% Cr, and the maximum negative value of SRO parameter was found to be only −0.025, while the experimental result at $T=705$ K is twice that and equals −0.05.[45] As the temperature of the simulation increases to values comparable to those used in experimental observations, short-range order becomes very weak and eventually vanishes. The difference of this magnitude is significant, and our results agree with the findings of Ref. 46 in that this raises doubts about the accuracy of DFT-CPA calculations.

In Fig. 6 we show the calculated first and the second nearest neighbor SRO parameters for temperature $T=750$ K, which is close to the temperature of the original experiment (705 K). In the original experiment,[45] the authors determined an average SRO parameter for the first- and the second-nearest neighbors, $\alpha_{1,2}=(8\alpha_1+6\alpha_2)/14$. The first and the second SRO parameters found in our simulations are very close to each other. The dashed line in Fig. 6 shows the lowest possible theoretical value of $\alpha_{1,2}$. For small concentrations of Cr, we found behavior similar to that observed in experiment: the negative value of parameters is very close to their theoretical minimum at 5% Cr. With increasing concentration, α_1, α_2, and their average $\alpha_{1,2}$ change sign at about 10.5% Cr. The difference is larger at 15% Cr, where our results are substantially higher than the experimental points, indicating that the degree of clustering of Cr atoms at this concentration and $T=750$ K predicted by our model is greater than that observed experimentally. The reasons for

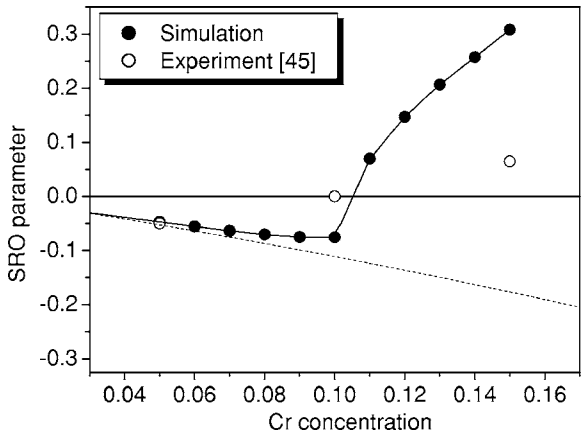

FIG. 6. The calculated averaged values of the first and the second Warren-Cowley SRO parameters in the FeCr solid solution shown as a function of Cr concentration at $T=750$ K. Open circles show experimental values taken from Ref. 45. The dashed line shows the lowest theoretically possible value of the attractive short-range order parameter $\alpha_{1,2}$.

this might be both the limited validity of the currently available set of CE coefficients and the metastable nature of the alloy investigated experimentally.

D. Cr clustering

As the concentration of Cr increases, Cr atoms start to cluster. Previously, the equilibrium size and the shape of precipitates were studied in the CE approximation for Al-Cu[48] and Al-Zn[49] alloys. In order to study clustering as a function of temperature and concentration, we defined "a Cr (Fe) cluster" as a set of two or more Cr (Fe) atoms connected to each other by the nearest-neighbor bonds. In this way individual chromium clusters are separated from each other by atoms of iron and might include two or more Cr atoms, and vice versa for the iron clusters. Using this definition it is possible to evaluate the number, the sizes, and the shapes of clusters in any equilibrium configuration. We investigated clustering occurring at several temperatures: 800, 1400, and 1600 K. For comparison, we also calculated the number and the size of clusters in a completely random Fe-Cr solution. In Fig. 7 we show the fraction of Cr atoms belonging to clusters (a) and the size of the largest Cr cluster (b) as functions of concentration. As expected, at low concentrations (less than 10%), clustering of Cr atoms is negligible. Above the 10% concentration, Cr atoms start forming large clusters at $T=800$ K. At higher temperatures, clustering is delayed until the Cr concentration reaches 20%. There is an important difference between clustering at temperatures of 1400 K and 1600 K. Both the ratio of clustered atoms and the largest cluster size calculated for $T=1600$ K and for the random distribution of atoms, are almost identical in the concentration range above 20% Cr. This confirms that at 1600 K the transition to complete miscibility has already taken place, as we have already deduced from the concentration dependence of the enthalpy of mixing in Sec. III B. On the other hand, the sizes of the largest clusters at $T=800$ K and $T=1400$ K for concentration exceeding 20% Cr converge toward each other. A similar

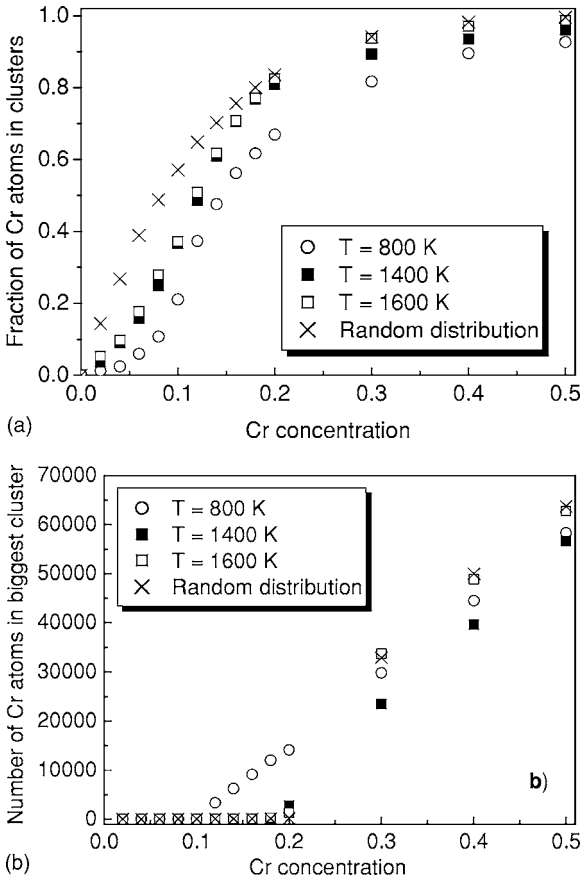

FIG. 7. The fraction of Cr atoms belonging to clusters (a) and the size of the largest Cr cluster (b) shown as functions of Cr concentration. For comparison, the same quantities are shown for a random distribution of Cr atoms.

behavior is observed for the ratio of Cr atoms in clusters, suggesting that in our model phase separation occurs above 10% Cr for $T=800$ K and above 20% Cr for $T=1400$ K.

Clustering of iron atoms in the chromium-rich region of the phase diagram differs dramatically from Cr clustering in the iron-rich region. Clustering of Fe starts at the lowest concentrations for all temperatures, as can be seen in Fig. 8(a), where we show the fraction of Fe atoms belonging to clusters in the Cr-rich regions. For all the concentrations and temperatures, the number of iron atoms in clusters is higher than in the case of a random distribution of atoms corresponding to the same concentration. The same striking difference is illustrated by the size of the largest cluster forming in the system, as shown in Fig. 8(b). Whereas on the iron-rich side the largest Cr cluster at 10% Cr includes only 16 atoms, the largest iron cluster at 10% Fe consists of more than 600 atoms at $T=1600$ K and of more than 5000 atoms at lower temperatures. This difference between clustering at the Fe-rich and Cr-rich ends of the composition range reflects the differences in the enthalpy of mixing (Figs. 1 and 5) for the iron- and the chromium-rich regions of the phase diagram.

We also evaluated the distribution of Cr cluster sizes for a number of temperatures and concentrations. In Fig. 9 the distribution of clusters as a function of their size is shown for

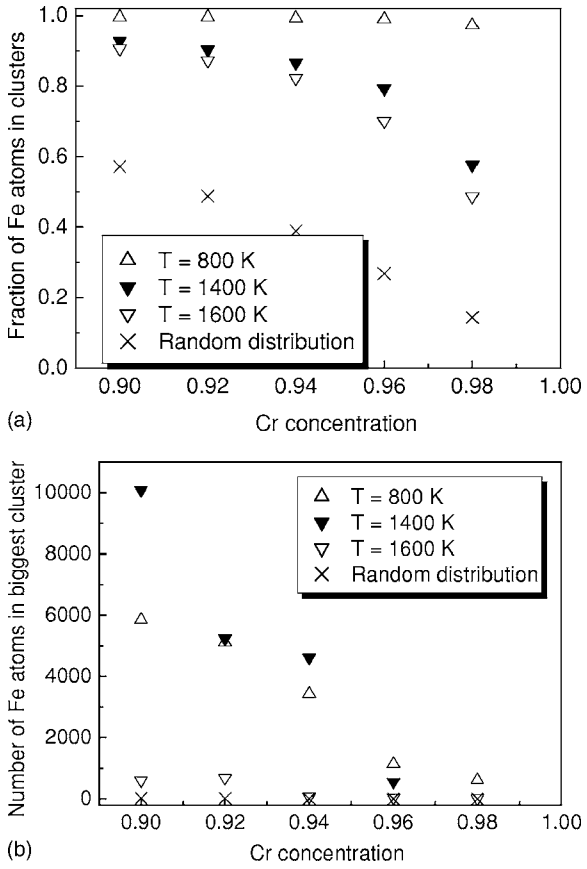

FIG. 8. The fraction of Fe atoms belonging to clusters (a) and the size of the largest Fe cluster (b) shown as functions of Cr concentration. For comparison, the same quantity is shown for a random distribution of Fe atoms.

10% Cr concentration, i.e., in the concentration region where clustering is negligible and the biggest cluster consists of only 16 Cr atoms. For all the temperatures studied here the number of clusters is lower than the number of clusters of the same size in a random distribution of atoms, and this difference increases as the cluster size increases. Note that at a

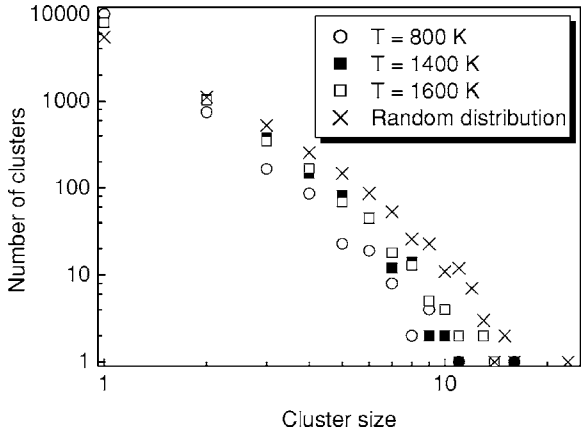

FIG. 9. The number of Cr clusters in the simulation cell plotted as a function of the size of a cluster for 10% Cr concentration. For comparison, crosses show the same quantity evaluated for a random distribution of Cr atoms.

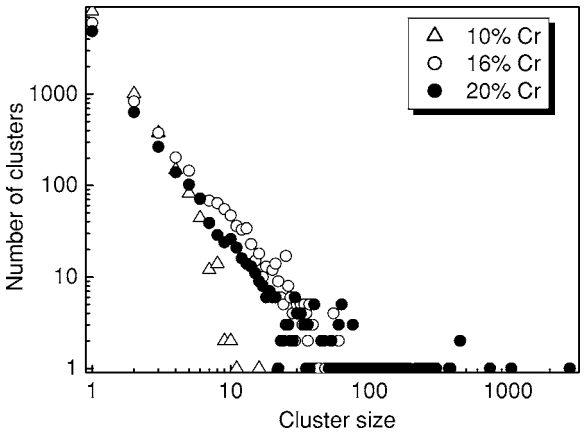

FIG. 10. The number of Cr clusters in the simulation cell plotted as a function of the size of a cluster for $T=1400$ K for 10%, 16%, and 20% Cr.

lower temperature $T=800$ K the number of large-size clusters is smaller than at a higher temperature. This is because at lower temperatures the contribution of the configurational entropy to the free energy is smaller and less significant for the cluster distribution, and the structure of the alloy is dominated to a greater extent by the energy (i.e., the enthalpy of mixing) term, favoring the dissolution of Cr atoms in the Fe matrix.

Once the level of concentration of 10–20%, depending on temperature, is reached, the equilibrium distribution includes large clusters of Cr. In Fig. 10, we show how the size distribution of clusters at temperature $T=1400$ K changes with increasing Cr concentration from 10% to 20%. At 16% Cr, where the biggest cluster consists of 129 atoms, the size distribution already differs from the distribution at 10% Cr, especially for clusters consisting of more than ten atoms. At 20% Cr, the size distribution is similar to that at 16% Cr, but the system includes also much larger clusters (the biggest cluster consists of 2789 atoms). For both the 16% and 20% Cr concentrations and for clusters containing fewer than 20 atoms the distribution of cluster sizes can be approximated by a power law with the exponent close to −2

$$N(s) \propto s^b, \tag{6}$$

where $N(s)$ is the number of clusters of size s. According to our calculation $b=-2.01$ for 16% Cr and $b=-2.13$ for 20% Cr.

Finally, we have investigated the shapes of larger Cr clusters. In Fig. 11, snapshots of Cr clusters are shown for several temperatures and concentrations. Note that single Cr atoms are not shown, so that the system includes Cr clusters and an α-phase consisting of the matrix of iron atoms with single Cr atoms dissolved in it. The concentration of Cr in the α-phase is approximately 8%. At $T=0$ K and 10% Cr, the lowest-energy configuration consists of one large Cr cluster with Cr-Fe interfaces being parallel to the [110] planes [Fig. 11(a)]. Note that the distance between the Cr and Fe planes is the largest for the interfaces of the [110] type. Using the CE approximation, we calculated the interfacial energy for the three coherent interfaces ([110], [100], and [111]) and found

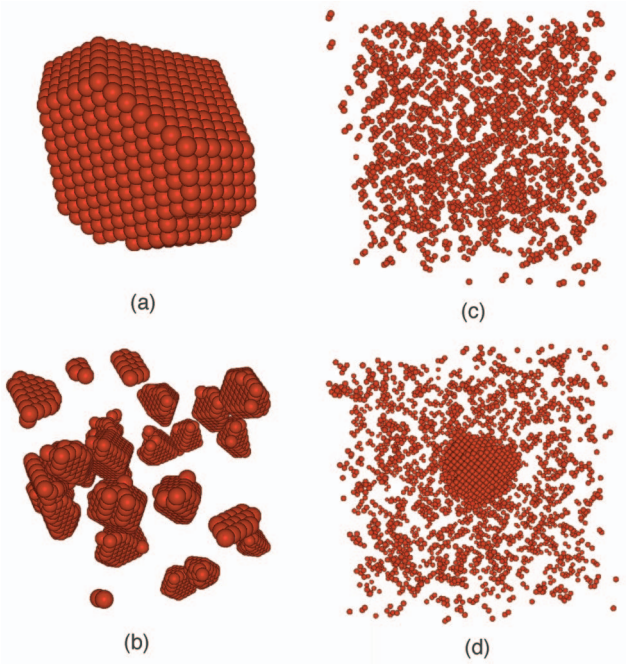

FIG. 11. (Color) Cr clusters in iron. Note that single Cr atoms are not shown, so that the system includes Cr clusters and α-phase consisting of the matrix of iron atoms with single Cr atoms dissolved in it. The concentration of Cr in the α-phase is approximately 8%. 10% Cr, $T=0$ (10a), 10% Cr, $T=200$ K (10b), 10% Cr, $T=800$ K (10c), 11% Cr, $T=800$ K (10d).

it to be lowest in the [110] case (2.97 meV/Å^2, compared to 9.7 meV/Å^2 for the [111] and 13.36 meV/Å^2 for the [100] interface). The shape of clusters remains the same at $T=200$ K [Fig. 11(b)], but now the system consists of a number of smaller clusters. At $T=800$ K and 10% Cr clustering does not seem to occur [Fig. 11(c)], but after increasing the Cr concentration by only 1%, we find a large cluster [Fig. 11(d)]. Note that unlike the case of low temperatures, the boundary of this cluster is not very well defined. Also, many smaller clusters continue to exist alongside the big cluster.

E. Semi-grand-canonical ensemble simulations

As we have seen in Sec. III B, the behavior of the enthalpy of mixing indicates that the transition to complete miscibility in the entire range of concentrations occurs between 1400 K and 1600 K in the CE approximation for the set of coefficients adopted in this study. The temperature corresponding to the top of the miscibility gap of a solid solution (the consolute temperature) may be also estimated by another method that requires calculating the difference between the chemical potentials of the two species, as described in Sec. II B. A miscibility gap exists if the free energy of the system plotted as a function of concentration has two minima corresponding to the two coexisting phases. Above the consolute temperature, the free energy has only one minimum, so that its derivative with respect to concentration increases monotonically in the entire range of concentrations.[21] Using formula (3) relating the derivative of the free energy to the difference in the chemical potentials,

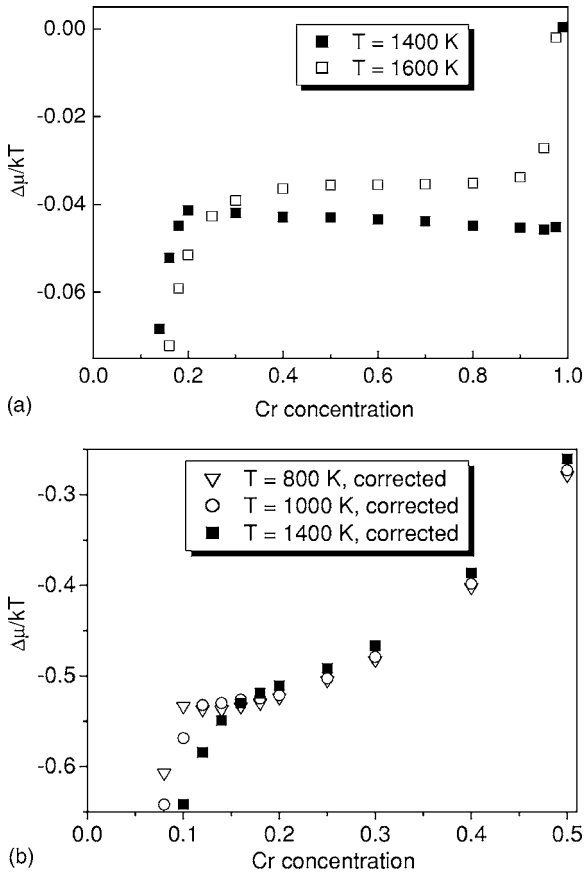

FIG. 12. The difference between chemical potentials of chromium and iron $\Delta\mu=\mu_{Cr}-\mu_{Fe}$ plotted as a function of Cr concentration for several temperatures. Curve (a) was not corrected for the vibrational entropy effects, while curve (b) includes this correction evaluated on the basis of data taken from Ref. 52.

the disappearance of the miscibility gap can be estimated from the behavior of $\Delta\mu=\mu_{Cr}-\mu_{Fe}$ versus Cr concentration. The results for $\Delta\mu$ obtained in the semi-grand-canonical ensemble simulations are shown in Fig. 12(a) for temperatures $T=1400$ K and $T=1600$ K. At $T=1600$ K $\Delta\mu$ increases for all concentrations (although the rate of the increase is very small between 50% and 80% Cr), indicating the formation of full solid solution, while at $T=1400$ K there is a region of concentrations where $\Delta\mu$ decreases with increasing Cr concentration, suggesting that at this temperature there is a miscibility gap. This suggests that the consolute temperature is very close to 1600 K and thus is overestimated in the simulations in comparison with experiment. Neglecting the presence of the σ-phase, CALPHAD gives the value of 895 K (Ref. 50) for the consolute temperature. The reason for the discrepancy may be taking insufficient account of the vibrational degrees of freedom in the CE approximation, as well as the limitations of the current set of CE coefficients.

The significance of the vibrational entropy contribution to the thermodynamics of alloys and solid solutions was discussed in Ref. 51. For solids, the "fast" vibrational degrees of freedom can be separated from the "slow" configurational ones in calculating the partition function, and accordingly the free energy can be decomposed into configurational and vibrational parts [see the discussion in Secs. II B and II C in

Ref. 51, in particular the formula (3) there]. If the temperature of interest is higher than the Debye temperature (which is the case here, as the Debye temperatures of Fe and Cr are 420 K and 460 K, respectively), the vibrational energy is determined by the equipartition theorem and is independent of the concentration. Then, the lattice vibrations mainly influence phase stability through their entropic contribution

$$\Delta G_{vibr} = -T\Delta S_{vibr}. \quad (7)$$

The difference in the chemical potentials adjusted to the vibrational effects can then be found [see formula (3)] by differentiating ΔS_{vibr} with respect to the Cr concentration and subtracting the result from the configurational part of $\Delta\mu$ obtained using (4). In order to take into account the vibrational entropy we employed the results of calculations of phonon spectra and associated entropy by Fultz *et al.*,[52] who used results of neutron inelastic-scattering experiments on Fe, Cr, and three Fe-Cr alloys. These experiments give information on the phonon density of states and make it possible to calculate the vibrational entropy of mixing. We fitted the data for ΔS_{vibr} treated as a function of concentration with a fourth-order polynomial. The corrected results for temperatures $T=1400$ K, $T=1000$ K, and $T=800$ K are shown in Fig. 12(b). At $T=1400$ K the corrected $\Delta\mu$ increases for all the concentrations, and from the figure the consolute temperature now can be estimated as being close to 1000 K, which is substantially lower than for the uncorrected results and in much better agreement with the CALPHAD predictions. Better agreement between theory and available experimental data might be achieved by improving the cluster expansion set of coefficients and also by taking into account the vibrational part of the enthalpy and its dependence on temperature. Also, in future the calculations in a semi-grand-canonical ensemble may be supplemented by simulations performed using a transmutational ensemble.[53,54] In this ensemble, the difference in the chemical potentials between the two species is a parameter of the simulation, and a transformation of one species into another is explicitly allowed. Then, the vibrational corrections to the $\Delta\mu$ can be introduced during the simulation.

IV. DISCUSSION AND CONCLUSIONS

In this paper we described a Monte Carlo study of thermodynamical properties of FeCr alloys for the entire range of Cr concentrations. We used a set of cluster expansion coefficients that are particularly accurate in the range of low Cr concentration (up to 20%). Our results prove the usefulness and the suitability of a combined cluster expansion and Monte Carlo approach for studying phase transformations occurring in iron-chromium alloys. MC simulations involving small supercells were used to find the most stable configurations. The set of CE coefficients consisting of 12 clusters was first validated by comparing the predicted values of enthalpies with the available experimental data and with DFT calculations, and then used in large-scale MC simulations.

This study of the concentration dependence of the enthalpy of mixing confirmed earlier predictions that in the range of concentrations below 12% Cr the enthalpy of mixing was negative. In the cluster expansion approximation adopted in this paper the lowest enthalpy of mixing corresponds to the Fe-6.25%Cr configuration. The value of the enthalpy of mixing is −4.8 meV/atom in the CE approximation compared to −6.5 meV/atom found in a DFT calculation. The lowest mixing enthalpy configuration found by DFT calculation so far is the Fe7.41%Cr structure shown in Fig. 3(b), and the mixing enthalpy of this configuration is −8.4 meV/atom (the CE value is −3.0 meV/atom).

MC simulations performed for large systems show that the negative enthalpy of mixing related to the negative enthalpy of mixing below 12% Cr persists even in the limit of very high temperature. This is accompanied by a narrowing of the concentration range corresponding to a negative enthalpy of mixing. This result is significant since it is accessible to a direct experimental verification. For example, even at $T=1600$ K the enthalpy of mixing remains negative up to 7% Cr. The occurrence of the γ-loop at this temperature makes experimental studies impossible, but we see no difficulty with performing experimental observations at a lower temperature. Negative enthalpy of mixing at small Cr concentrations results in a substantial asymmetry of the α-α' phase diagram: phase separation begins at the smallest concentrations of Fe in the α'-phase, but in the α-phase, at small Cr concentrations chromium atoms tend to stay separated from each other, and clustering starts only at 10%, or even higher, Cr concentration and the occurrence of clustering depends on temperature.

Our simulations also confirm the change in the sign of the short-range order parameters occurring in the low-Cr region, which agrees with experimental data. We find that the sign of the first and second SRO parameters changes at about 10% Cr, in agreement with the neutron-scattering experiments.[45] Results presented here improve agreement with experiment in the negative SRO range in comparison with the recent DFT-CPA-based atomistic simulations.[46]

Above a certain threshold concentration, which is a function of temperature, Cr atoms cluster. We have investigated the effect of equilibrium clustering as a function of temperature and concentration, and compared it with the case of a random distribution of Cr atoms. Clustering starts at 10% Cr at $T=800$ K. At higher temperatures, configurational entropy delays clustering, and in particular, at $T=1400$ K it starts at 20% Cr. At an even higher temperature, $T=1600$ K, both the ratio of clustered atoms and the largest cluster size at high Cr concentrations almost coincide with the values found for the case of random solid solution, confirming that the system is above the α-α' miscibility gap. We have also studied clustering of iron atoms in the Cr-rich region. In contrast to the iron-rich region, clustering occurs for all, including the smallest, Fe concentrations. This difference reflects the difference in the concentration dependence of the enthalpy of mixing in the two regions.

We have also investigated the shape and the size distribution of the Cr clusters. We found that the Cr-Fe interfaces are parallel to the [110] planes, where the distance between the neighboring planes is the largest. The size of the clusters is distributed according to a power law, and the distribution changes substantially in the concentration range where clustering of Cr atoms occurs.

The new data describing the behavior of the enthalpy and the difference of chemical potentials as functions of concentration may be used in calculating the phase diagram of the system. We found that the consolute temperature of the α-α' phase diagram in the CE approximation lies between 1400 and 1600 K. This is higher than the values predicted by CALPHAD, and the disagreement is partially attributable to the absence of a vibrational entropy term in the cluster expansion and the limitations of the current set of CE coefficients. The incorporation of experimental data on the vibrational entropy of the Fe-Cr system[52] improves the agreement between our results and those of CALPHAD.

Our MC simulations provided information about the short-range order, clustering, and thermodynamic properties of the Fe-Cr system, and proved the validity of a combined CE and MC approach. As a next step, the results obtained so far can be applied to study the phase diagram of Fe-Cr containing defects. The time dependence and the patterns of evolution of cluster formation can be addressed by combining the CE approach with kinetic Monte Carlo simulations. The rate of cluster growth, the time dependence of their shape, and ripening can all be studied using this model. Current simulations can also be used for investigating the behavior of Fe-Cr subjected to an external driving force, namely, ballistic mixing, and hence can be extended to the important case of oxide-dispersion-strengthened steels. The theoretical framework for modeling irradiation via random changes of atomic configuration is available[55] and can now be implemented using the cluster expansion Monte Carlo algorithm. This will allow investigation of the resistivity recovery curves and comparison of them with the available experimental data.

While the CE is most useful for studying low-energy configurations and systems where the configurational disorder is dominant compared to the vibrational disorder, the main limitation of the present work is the neglect of vibrational contributions to the entropy and the free energy as well as the modification of the magnetic contributions to the ECIs as a function of temperature. This makes the present work less suitable for evaluating the miscibility gap at the top of the phase diagram, because that is where the vibrational contributions and magnetic excitations are most important. The current set of CE coefficients was created using the DFT data modeling of mainly the low-Cr-concentration region and this needs to be improved, especially in the Cr-rich region, using an extended DFT database. Currently, we are developing an improved set of cluster expansion coefficients which should give better agreement between the DFT results and the CE predictions in the entire range of Cr concentration.

Summarizing, we have presented a Monte Carlo study of the Fe-Cr system based on the cluster expansion of the configurational contributions to the enthalpy of the alloy. We found that negative enthalpy of mixing at low Cr concentrations results in a substantial asymmetry of the α-α' phase diagram, with a substantial degree of phase separation occurring at the Cr-rich end of the diagram, while in the α-phase chromium atoms tend to stay separated from each other, and clustering starts only at 10% or even higher Cr content, depending on temperature. The results provide deeper insight into the microscopic mechanisms of clustering, short-range order, and thermodynamic properties in this system, especially in the limit of low Cr concentration, and can be used in future studies of the phase diagram as well as the nonequilibrium behavior of this technologically important system.

ACKNOWLEDGMENTS

We would like to thank A. P. Miodownik, Magdalena and Alfredo Caro, and Dorothy Duffy for valuable and stimulating discussions. Work at UKAEA was funded by the EXTREMAT Integrated Project, by the Engineering and Physical Sciences Research Council (EPSRC), and by EURATOM through task TTMS-007-01. Work at Belfast and at Oxford was funded through an EPSRC consortium on fusion materials modeling.

*Corresponding author. Electronic address: Mikhail.Lavrentiev @ukaea.org.uk

[1] I. Cook, Nat. Mater. **5**, 77 (2006).
[2] S. L. Dudarev and P. M. Derlet, J. Phys.: Condens. Matter **17**, 7097 (2005).
[3] G. Liu, D. Nguyen-Manh, B. G. Liu, and D. G. Pettifor, Phys. Rev. B **71**, 174115 (2005).
[4] D. Nguyen-Manh, A. P. Horsfield, and S. L. Dudarev, Phys. Rev. B **73**, 020101(R) (2006).
[5] D. Nguyen-Manh and S. L. Dudarev, Mater. Sci. Eng., A **423**, 74 (2006).
[6] G. R. Odette, T. Yamamoto, H. J. Rathbun, M. Y. He, M. L. Hribernik, and J. W. Rensman, J. Nucl. Mater. **323**, 313 (2003).
[7] E. E. Bloom, S. J. Zinkle, and F. W. Wiffen, J. Nucl. Mater. **329-333**, 12 (2004).
[8] L. K. Mansur, A. F. Rowcliffe, R. K. Nanstad, S. J. Zinkle, W. R. Corwin, and R. E. Stoller, J. Nucl. Mater. **329-333**, 166 (2004).
[9] S. J. Zinkle, Phys. Plasmas **12**, 058101 (2005).
[10] J.-O. Andersson and B. Sundman, CALPHAD: Comput. Coupling Phase Diagrams Thermochem. **11**, 83 (1987).
[11] *Binary Alloy Phase Diagrams*, 2nd ed., edited by T. B. Massalski, (ASM International, Materials Park, OH, 1990), Vols. 1–3.
[12] M. H. Mathon, Y. de Carlan, G. Geoffroy, X. Averty, A. Alamo, and C. H. de Novion, J. Nucl. Mater. **312**, 236 (2003).
[13] *Group IV: Physical Chemistry*, Vol. 19, *Thermodynamic Properties of Inorganic Materials*, Subvolume B: Binary Systems, Part 2: Binary Systems from B-C to Cr-Zr, Landolt-Bornstein (Springer, Berlin, 2004).
[14] J. M. Sanchez, F. Ducastelle, and D. Gratias, Physica A **128**, 334 (1984).
[15] A. Zunger, in *Statics and Dynamics of Alloy Phase Transformations*, edited by P. E. A. Turchi and A. Gonis, Proceedings of the NATO ASI (Plenum Press, New York, 1994), p. 361.
[16] R. Drautz, Ph.D. Thesis, Stuttgart, 2003.
[17] R. Drautz and M. Fähnle, Phys. Rev. B **69**, 104404 (2004).
[18] R. Drautz, A. Díaz-Ortiz, M. Fähnle, and H. Dosch, Phys. Rev.

Lett. **93**, 067202 (2004).
[19] A. Díaz-Ortiz, R. Drautz, M. Fähnle, and H. Dosch, J. Magn. Magn. Mater. **272-276**, 780 (2004).
[20] J. A. Purton, G. D. Barrera, M. B. Taylor, N. L. Allan, and J. D. Blundy, J. Phys. Chem. B **102**, 5202 (1998).
[21] N. L. Allan, G. D. Barrera, M. Yu. Lavrentiev, I. T. Todorov, and J. A. Purton, J. Mater. Chem. **11**, 63 (2001).
[22] N. I. Metropolis, A. W. Rosenbluth, M. N. Rosenbluth, A. H. Teller, and E. Teller, J. Chem. Phys. **21**, 1087 (1953).
[23] M. Yu. Lavrentiev, N. L. Allan, G. D. Barrera, and J. A. Purton, J. Phys. Chem. B **105**, 3594 (2001).
[24] M. Yu. Lavrentiev, J. A. Purton, and N. L. Allan, Am. Mineral. **88**, 1522 (2003).
[25] M. Yu. Lavrentiev, W. van Westrenen, N. L. Allan, C. L. Freeman, and J. A. Purton, Chem. Geol. **225**, 336 (2006).
[26] F. M. Marquez, C. Cienfuegos, B. K. Pongsai, M. Yu. Lavrentiev, N. L. Allan, J. A. Purton, and G. D. Barrera, Modell. Simul. Mater. Sci. Eng. **11**, 115 (2003).
[27] R. Hojvat de Tendler, R. M. Fracchia, M. E. Pepe, M. Yu. Lavrentiev, and M. R. Soriano, J. Argentine Chem. Soc. **93**, 137 (2005).
[28] J. A. Purton, M. Yu. Lavrentiev, N. L. Allan, and I. T. Todorov, Phys. Chem. Chem. Phys. **7**, 3601 (2005).
[29] R. Drautz and A. Díaz-Ortiz, Phys. Rev. B **73**, 224207 (2006).
[30] A. Díaz-Ortiz, R. Drautz, M. Fähnle, H. Dosch, and J. M. Sanchez, Phys. Rev. B **73**, 224208 (2006).
[31] A. Díaz-Ortiz, R. Drautz, M. Fähnle, and H. Dosch (unpublished).
[32] T. P. C. Klaver, R. Drautz, and M. W. Finnis, Phys. Rev. B **74**, 094435 (2006).
[33] D. Nguyen-Manh, UKAEA Fusion Report No. F/PL/L2.M1, Nov 2005 (unpublished).
[34] D. Nguyen-Manh, M. Yu. Lavrentiev, and S. L. Dudarev, in *Proceedings of the 3rd International Conference on Multiscale Materials Modelling* (P. Gumbsch, Freiburg, Germany, 2006), pp. 767–770; D. Nguyen-Manh, M. Yu. Lavrentiev, and S. L. Dudarev (to be published).
[35] A. Pasturel, C. Colinet, D. N. Manh, A. T. Paxton, and M. van Schilfgaarde, Phys. Rev. B **52**, 15176 (1995).
[36] C. Colinet, A. Pasturel, D. N. Manh, D. G. Pettifor, and P. A. Miodownik, Phys. Rev. B **56**, 552 (1997).
[37] K. Kawasaki, in *Phase Transitions and Critical Phenomena*, edited by C. Domb and M. S. Green (Academic, New York, 1972), Vol. 2, p. 443.
[38] K. Binder and D. W. Heermann, *Monte Carlo Simulation in Statistical Physics*, 2nd ed. (Springer, Berlin, Heidelberg, 1992).
[39] D. A. Kofke and E. D. Glandt, Mol. Phys. **64**, 1105 (1988).
[40] D. Frenkel and B. Smit, *Understanding Molecular Simulation*, 2nd ed. (Academic Press, San Diego, CA, 2002).
[41] P. Olsson, I. A. Abrikosov, L. Vitos, and J. Wallenius, J. Nucl. Mater. **321**, 84 (2003).
[42] P. Olsson, I. A. Abrikosov, and J. Wallenius, Phys. Rev. B **73**, 104416 (2006).
[43] N. Saunders and A. P. Miodownik, *CALPHAD: A Comprehensive Guide*, edited by R. W. Cahn (Pergamon Materials Series, Oxford, New York, 1998).
[44] M. Hennion, J. Phys. F: Met. Phys. **13**, 2351 (1983).
[45] I. Mirebeau, M. Hennion, and G. Parette, Phys. Rev. Lett. **53**, 687 (1984).
[46] A. Caro, D. A. Crowson, and M. Caro, Phys. Rev. Lett. **95**, 075702 (2005).
[47] P. Olsson, I. A. Abrikosov, L. Vitos, and J. Wallenius, J. Nucl. Mater. **321**, 84 (2003).
[48] C. Wolverton, Philos. Mag. A **79**, 683 (1999).
[49] S. Müller, C. Wolverton, L.-W. Wang, and A. Zunger, Acta Mater. **48**, 4007 (2000).
[50] A. P. Miodownik, private communication.
[51] A. van de Walle and G. Ceder, Rev. Mod. Phys. **74**, 11 (2002).
[52] B. Fultz, L. Anthony, J. L. Robertson, R. M. Nicklow, S. Spooner, and M. Mostoller, Phys. Rev. B **52**, 3280 (1995).
[53] B. Dünweg and D. P. Landau, Phys. Rev. B **48**, 14182 (1993).
[54] M. Laradji, D. P. Landau, and B. Dünweg, Phys. Rev. B **51**, 4894 (1995).
[55] A. C. Lund and C. A. Schuh, Phys. Rev. Lett. **91**, 235505 (2003).